

# Morphological Transitions in an I<sub>2</sub>S Simple Graft Block Copolymer: From Folded Sheets to Folded Lace to Randomly Oriented Worms at Equilibrium

Darrin J. Pochan and Samuel P. Gido\*

Department of Polymer Science and Engineering, University of Massachusetts at Amherst, Amherst, Massachusetts 01003

Stergios Pispas† and Jimmy W. Mays

Department of Chemistry, University of Alabama at Birmingham, Birmingham, Alabama 35294

Received January 25, 1996; Revised Manuscript Received April 25, 1996<sup>®</sup>

**ABSTRACT:** A new equilibrium morphology consisting of randomly oriented wormlike micelles dispersed in a continuous matrix is observed in a neat, strongly segregated I<sub>2</sub>S simple graft block copolymer. The equilibrium nature of the worm phase is determined via a set of selective solvent casting and prolonged annealing experiments. Transmission electron microscopy (TEM) experiments on quenched samples allow a unique opportunity to directly observe the transition of a kinetically trapped, nonequilibrium folded-layer morphology, formed by casting the sample with a solvent selective for polyisoprene (PI), into the equilibrium, randomly oriented worm phase through an intermediate folded-lace morphology. The folded-lace intermediate is similar to the “mesh” structure previously observed by Hashimoto et al. in starblock/homopolymer blends.<sup>1</sup> The simple graft block copolymer, formed by grafting a single polystyrene (PS) chain onto the center of a polyisoprene backbone, introduces a 2:1 PI/PS arm number asymmetry in the microphase separated state. The 0.81 volume fraction of the PS graft is theoretically predicted<sup>2</sup> to be the first volume fraction of graft large enough to force the two PI arms per molecule to the concave side of the PI/PS interface in the microphase separated state. This unique volume fraction, coupled with the novel graft architecture, seems to frustrate the system from choosing a lattice during the microphase separation process.

## Introduction

By synthetically altering the architecture of block copolymers to form grafts, one is able to divorce the strongly segregated phase behavior of amorphous block copolymers from its strict dependence on the relative volume fraction of the respective blocks. While the phase behavior of linear, conformationally symmetric diblocks is solely dependent on the relative volume fractions of the constituent blocks, manipulation of architecture allows additional control of the solid state, equilibrium morphology. By utilizing an A<sub>2</sub>B, or “Y”-shaped, simple graft architecture, one is able to produce phase behavior unobtainable with linear diblock architecture at the same volume fractions. The molecules studied here are formed by connecting two polyisoprene chains to a terminally difunctional polystyrene chain, hence forming an I<sub>2</sub>S molecule. The 2:1 arm number asymmetry of PI to PS in the microphase separated state, as shown in Figure 1, has been found to skew the volume fraction dependence of the strongly segregated phase behavior to much higher PS volume fractions than found in diblock architecture.<sup>3</sup> In the Pochan et al. I<sub>2</sub>S simple graft morphological survey, an intriguing structure is observed at one particular composition in which the two PI blocks are just short enough to be confined to the concave side of the interface. This structure, formed by the neat graft block copolymer, consists of randomly oriented wormlike micelles (hereafter named the ROW phase) with PI in the cores and the grafted PS block material forming the continuous matrix. While Kinning, Winey, and Thomas have

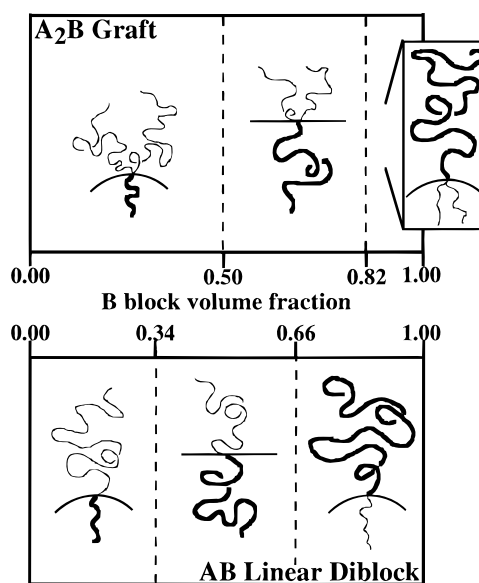


**Figure 1.** Schematic of the A<sub>2</sub>B, or “Y”, molecular architecture in the microphase separated state. The two A chains per molecule are calculated<sup>2</sup> to reside on the convex side of a curved A/B interface until much higher volume fractions than what is experimentally found in diblock architecture.<sup>26</sup> A curved A/B interface generically represents spherical, cylindrical, and bicontinuous morphologies while the flat interface represents a lamellar morphology.

reported a similar wormlike micelle phase in blends of diblock copolymers with homopolymers,<sup>4</sup> this structure has not been previously observed in neat block copolymers. In ABC triblocks Jung et al. have synthesized molecules with designed packing frustrations specifically to suppress the formation of long-range order.<sup>5</sup> But the resulting bent cylinder “banana” morphologies still

\* To whom correspondence should be addressed.

† Present address: Department of Chemistry, University of Athens, Panepistimiopolis, Athens 157 71, Greece.

® Abstract published in *Advance ACS Abstracts*, June 15, 1996.

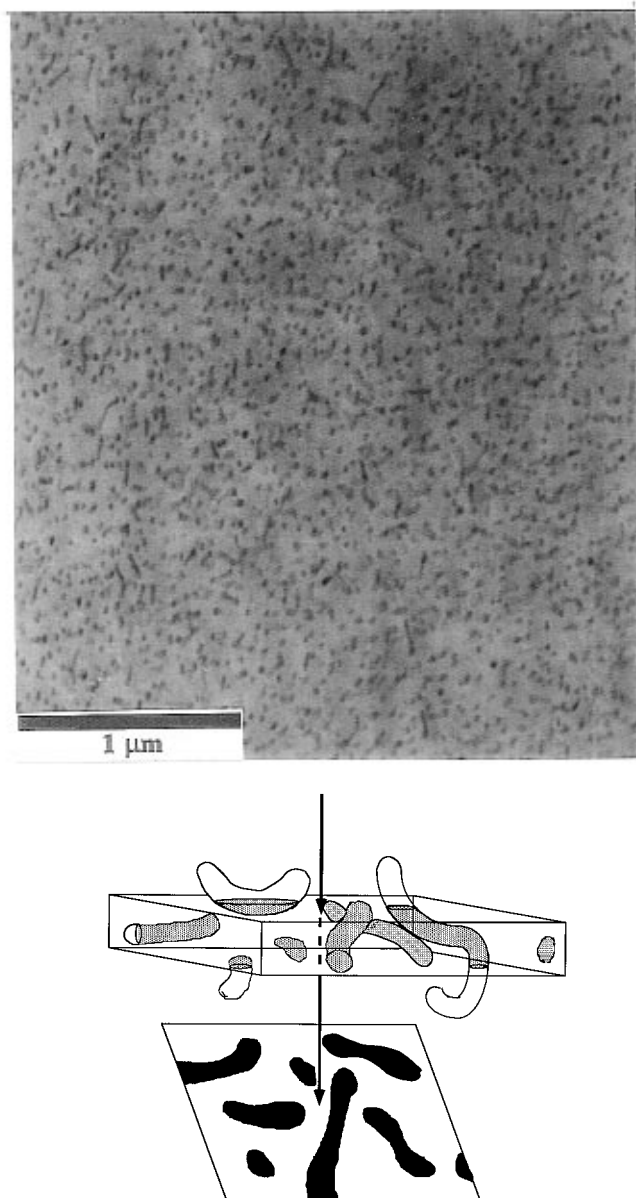


**Figure 2.** (a, top) TEM micrograph of toluene-cast I<sub>2</sub>S-81 annealed at 120 °C for 1 week showing randomly oriented, dark PI wormlike micelles embedded in the PS graft matrix. (b, bottom) Schematic showing the resultant 2-D TEM projection through a microtomed section of the randomly oriented, wormlike micelles.

form small grainlike regions of coherent domain orientation. In contrast, the ROW phase which we observe in the I<sub>2</sub>S system is completely random in orientation. Figure 2a shows a transmission electron microscopy (TEM) image of this morphology which appears as a random pattern of dark OsO<sub>4</sub> stained PI dots and short, often curved, line segments in a lighter PS matrix. The shape of a wormlike micelle projected in two dimensions is highly dependent on its orientation in three dimensions with respect to the incident electron beam. Figure 2b illustrates how TEM projections from a thin microtomed section of the ROW phase results in this type of image. Figure 3, a and b, is a tilt series at a higher magnification of an ultrathin section of the toluene-cast ROW phase. Spherical-shaped projections of the PI micelles in Figure 3a, which accompany more elongated wormlike structures, are merely projections perpendicular to thin cross sections of the worm micelles. After 40° of tilt in Figure 3b all of the PI micelles elongate

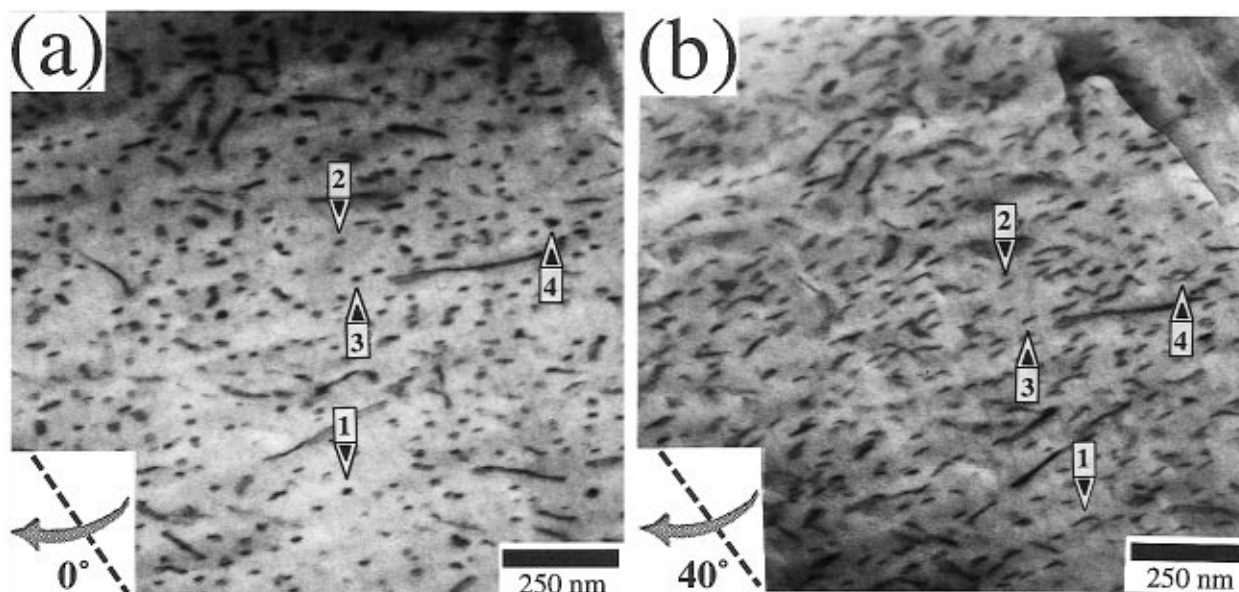
perpendicular to the tilt axis, thus revealing the wormlike nature of the entire system.

Figure 1 illustrates the chain packing considerations inherent in the microphase separation of I<sub>2</sub>S or "Y"-shaped block copolymers. In the microphase separated state the two symmetric PI blocks are crowded on the same side of the PS/PI interface which leads to additional PI chain stretching. To compensate for the PI crowding, there is an increased tendency for the interface to curve away from the PI blocks. This convexity provides more volume closer to the interface to pack the two PI chains. The two PI chains prefer to be on the convex side of a curved interface to significantly lower PI volume fractions than one observes in the corresponding diblocks. Or, looking at the situation from the point of view of the single PS graft, the windows in which the various morphologies are observed are shifted to higher volume fractions of the PS block.<sup>2</sup> Therefore, the morphology diagram, as shown in Figure 4, is markedly asymmetrical with respect to the two-component volume fractions.

The diagram is generic in that within the parameter  $\epsilon = (n_a/n_b)(l_a/l_b)^{1/2}$  different architectures and chain statistics are accounted for. The number of arms one chooses,  $n_a$  of A or  $n_b$  of B, can be varied. Also, differing chain statistics between blocks are represented in the square root ratios of  $l_a$  and  $l_b$  with  $l_i = V_i/R_i^2 = v_i/b_i^2$  where  $V_i$  and  $R_i$  are the molecular volume and radius of gyration of the respective blocks and  $v_i$  and  $b_i$  are the segment volume and Kuhn length of the respective blocks. If the constituent blocks are conformationally symmetric, then  $\epsilon$  is simply the ratio of the number of A and B arms in the molecule. For our PS-PI simple graft block copolymers,  $\epsilon \approx 1.8$  due to the statistical similarity of the PS and PI block materials.<sup>3</sup>

At  $\epsilon = 1$  the phase diagram models linear, AB diblock phase behavior with the phases being symmetric around  $\phi_b = 0.5$ . However, as one increases the arm number of one species relative to the other or varies the relative chain statistics of A and B, the phase behavior becomes extremely asymmetric with volume fraction. Hadjichristidis et al.<sup>6</sup> recently characterized the bulk phase behavior of three A<sub>2</sub>B block copolymers or "miktoarm" blocks. The asymmetry of the graft architecture forced two samples, a 37 vol % polystyrene "I<sub>2</sub>S" graft (isoprene backbone and a single styrene graft emanating from the middle of that backbone) and a 40 vol % (poly)styrene SIB miktoarm star (the rubbery phase consists of mixed isoprene and butadiene blocks), into cylindrical phases where the bulk morphology would be bicontinuous or lamellar, respectively, in diblock architecture analogs of the same molecular weight. All of the I<sub>2</sub>S samples in our morphological survey,<sup>3</sup> with PS graft volume fractions ranging from 0.08 to 0.89, displayed the shifted morphology behavior predicted by theory, except for  $\phi_s = 0.81$  which forms the ROW phase.

According to Milner's theory, for  $\epsilon \approx 1.8$ , at any  $\phi_s$  above approximately 0.82 the two PI blocks of the I<sub>2</sub>S molecule should reside on the concave side of the PS/PI interface (see Figure 3). This is in contrast to diblock architecture where above approximately  $\phi_s = 0.66$  a single PI block per diblock molecule is confined to the concave side of the interface.<sup>7,8</sup> Experimentally, our I<sub>2</sub>S sample at  $\phi_s = 0.81$ , hereafter referred to as I<sub>2</sub>S-81, is very close to this calculated transition of the PI chains to the concave side. However, instead of forming the theoretically calculated bicontinuous phase, the system microphase separates into the ROW phase. The lateral crowding of the two PI chains per molecule causes



**Figure 3.** TEM tilt series of toluene-cast ROW phase. (a) Ultrathin section at high magnification with 0° tilt. (b) Same area tilted 40° about the tilt axis. Several transitions from spherical to wormlike projections are marked with numbered arrows in the micrographs.

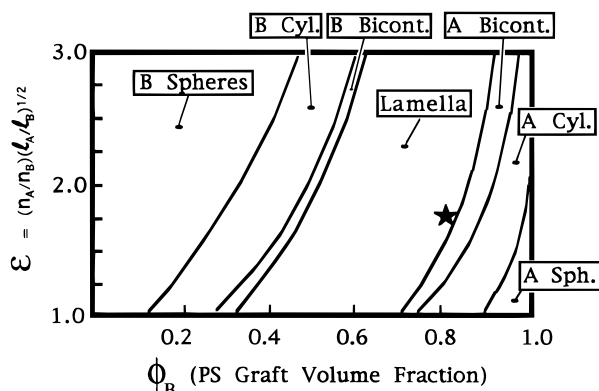


**Figure 4.** Theoretical phase diagram calculated by Milner.<sup>2</sup> The ★ at  $\epsilon \sim 1.80$  represents sample I<sub>2</sub>S-81 with  $\phi_s = 0.81$ .

increased chain stretching. The coupling of this crowding and subsequent stretching of the PI chains with the PI volume fraction being just low enough to force the PI chains to the concave side of the interface seems to frustrate the formation of a lattice in the system.

To test the equilibrium nature of the ROW phase in I<sub>2</sub>S-81, a series of selective solvent casting and extended annealing experiments were performed. The results support the equilibrium nature of the observed wormlike phase as well as provide an unusual opportunity to visualize several stages in the phase transition from a selective solvent cast, nonequilibrium layered morphology into the final, equilibrium ROW phase.

### Experimental Section

The synthesis of I<sub>2</sub>S block copolymers and the subsequent characterization of their molecular weights, polydispersities, and molecular architectures, including the  $\phi_s = 0.81$  sample of interest in this paper, are described in another publication.<sup>3</sup> The sample studied in this work, I<sub>2</sub>S-81, has a  $M_n = 89\,400$  and  $M_w$  of 90 800 as measured by membrane osmometry and LALLS, respectively.  $M_w/M_n = 1.04$  while the weight percent of PS is 0.84 as measured by SEC and SEC-UV, respectively. The PS graft is deuterated, so the  $\phi_s = 0.81$  was calculated at room temperature using  $\rho = 1.14$  and 0.91 g/mL<sup>3</sup> for d-PS and PI, respectively.

Solid films approximately 1 mm thick of the I<sub>2</sub>S block copolymer were slowly cast from 5 wt % polymer solutions in

cyclohexane, a selective solvent for PI, and dioxane, a selective solvent for PS. The solubility, or Hildebrand, parameters,  $\delta$ , are 17 MPa<sup>1/2</sup> for the predominantly 1,4-addition PI and 16.8 MPa<sup>1/2</sup> for cyclohexane while PS and dioxane have values of 18 and 20 MPa<sup>1/2</sup>, respectively, indicating the selectivity of cyclohexane for PI and dioxane for PS.<sup>9,10</sup> Casting was performed at room temperature, and the evaporation of solvent was controlled to form a solid film after 10–14 days. The films were given several more days at room temperature and atmospheric pressure and an additional several days under high vacuum at room temperature to allow residual solvent to evaporate.

Several pieces of both the cyclohexane and the dioxane cast films were annealed for 1 week at 120 °C in a high-vacuum oven. This annealing treatment is consistent with other experiments intended to drive samples cast from toluene, a nonpreferential solvent, further toward equilibrium.<sup>3</sup> This type of annealing experiment has been found to allow morphologies formed by solvent casting to slightly enlarge their long spacing and their average grain size, hence allowing the equilibrium lattice symmetry formed in the microphase separation process to simply reach an even more stable, minimum free energy state.<sup>4,11–13</sup>

Next, a set of prolonged annealing experiments at higher temperatures was performed on the cyclohexane prepared samples, both preannealed, as-cast samples and those which underwent the initial annealing treatment at 120 °C mentioned above. In our other work,<sup>3</sup> a series of seven I<sub>2</sub>S samples covering a wide range of volume fractions were found to resist oxidation after annealing in a high-vacuum oven for a period of 1 week at 120 °C. This was monitored via GPC experiments performed on the samples, including I<sub>2</sub>S-81 studied in this work, both before they were solvent cast and after they were annealed. The precasting and postannealing GPC traces were essentially identical, revealing highly narrow molecular weight distributions ( $PDI < 1.04$ ) with no detectable change in molecular weight. However, in an effort to eliminate any possible sample oxidation with prolonged annealing at higher temperatures, the cyclohexane-cast I<sub>2</sub>S-81 samples were first placed in glass ampules and evacuated on a high-vacuum line to approximately 0.1  $\mu$ m ( $10^{-4}$  Torr) pressure. Next, the entire system was purged with dehydrated, high-purity argon gas and subsequently evacuated. The evacuation and inert gas purge cycle was performed a total of three times per sample. The preparation was concluded by sealing the vials under high vacuum with a torch. The vacuum-sealed ampules were then annealed for 20 days at either 125 or 150 °C. Sample purity after the long annealing process was tested by recasting two

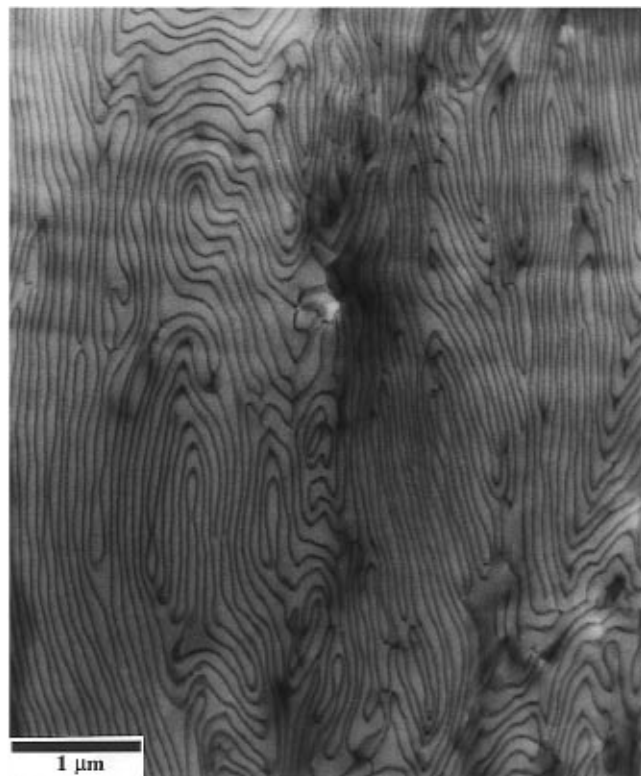


**Figure 5.** TEM micrograph of cyclohexane-cast I<sub>2</sub>S-81. The kinetically trapped, nonequilibrium morphology consists of alternating dark layers of PI and light layers of PS.

portions of the annealed I<sub>2</sub>S-81 sample, one in toluene and the other in cyclohexane. The phase behavior obtained in both cases was the same as found by using virgin material. This indicates the limited degradative and oxidative effect of the extended annealing process on the I<sub>2</sub>S-81 sample.

Estimated  $\chi N$  values for the system at elevated annealing temperatures of 125–150 °C range from 62 to 83 while at room temperature  $\chi N > 100$ ,<sup>14–16</sup> placing the system in the strong segregation limit (SSL) throughout the experiments. The large variability in  $\chi N$  values is due to the various methods employed in the measurement and calculation of  $\chi$ : (1) homopolymer phase behavior studies and (2) fitting of homogeneous diblock melt SAXS data to Leibler's calculated structure factor.<sup>17</sup> Compositional and molecular weight effects on  $\chi$  are neglected, and while the A<sub>2</sub>B architecture has been calculated to have a small enlarging effect on  $\chi N_s$  relative to linear diblocks of the same molecular weight,<sup>18</sup> any effect at the much lower temperatures employed in these experiments would be small and not take the system out of the SSL.

All samples for transmission electron microscopy (TEM) were microtomed in a Reichert-Jung cryoultramicrotome. Sections approximately 300–600 Å thick were cut with a Diatome cryo diamond knife at a sample temperature of –110 °C and a knife temperature of –90 °C. The sections were stained in OsO<sub>4</sub> vapors for 4 h. Bright-field TEM experiments were performed on a JEOL 100CX electron microscope operated at 100 kV accelerating voltage.

## Results and Discussion

Figure 5 is indicative of the lamellar-like morphology formed when I<sub>2</sub>S-81 is cast with cyclohexane, a selective solvent for PI. The samples producing this morphology were cast from solution but were not thermally annealed prior to microtoming and TEM imaging. As the microdomains of PS and PI form during the casting from cyclohexane, the solvent is partitioned unequally between the microdomains. Therefore, the PI volume fraction is effectively larger at the point of PS microphase separation, pushing the morphology into the

lamellar region of the I<sub>2</sub>S phase diagram. When the remaining solvent evaporates from the PI phase, the neat I<sub>2</sub>S block copolymer is kinetically trapped at room temperature in a nonequilibrium lamellar phase.

It is interesting to note that the lamellar microdomains in Figure 5 differ somewhat in morphology from lamellar structures produced in PS–PI block copolymers by cooling from the melt or casting from a nonpreferential solvent such as toluene. The morphology of the cyclohexane cast samples resembles sheets of cloth that have been folded back and forth. We postulate that this folded sheet morphology arises because the block copolymer in selective solvent microphase separates by first forming sheetlike micelles with solvent-poor PS layers separated by solvent-rich PI layers. These sheetlike micelles initially may be separated by a fair amount of solvent. However, when the cyclohexane is removed to produce the kinetically trapped morphology shown in Figure 5, the previously formed sheetlike micelles compact to fill space and, in so doing, may fold back and forth.

Annealing experiments allowed the kinetically trapped, folded-sheet lamellar structure to relax into its equilibrium structure, which we postulate to be the ROW phase. The folded lamella cyclohexane-cast samples which were annealed at 120 °C for 1 week transformed into an intermediate structure between the folded-sheet lamellar structure and the (assumed to be) equilibrium worm phase. This quenched intermediate morphology, which we refer to as folded lace, is shown in Figure 6a–c. The PI layers of the folded lamella are observed to be perforated by numerous channels connecting the PS layers on either side. Figure 6a is a more global micrograph revealing the similarity of the folded-lace microstructure to the unannealed lamellar morphology in Figure 5. Figure 6b is an enlargement of a projection parallel with the layers of the folded-lace structure. The dark spots within the dark PI layers are projections along the axes of the PI struts which constitute the lace structure. Figure 6c is a projection more normal to the lacy PI layers displaying the characteristic lace microstructure within a PI layer. The hole size of the lace seems to vary somewhat throughout the layers indicative of the intermediate, nonequilibrium nature of the structure. The observation of this intermediate morphology allows direct insight into the relaxation mechanism of the kinetically trapped, nonequilibrium structure into its final, equilibrium form.

This transition can best be explained by employing the idea that the block copolymer molecular architecture and volume fractions prescribe a natural or preferred interfacial curvature. This concept has been widely used in modeling the structures of micelles and microemulsions involving small molecule amphiphiles.<sup>19–21</sup> In the strong segregation limit (SSL) the preferred interfacial curvature determines the shape of the Gaussian wedge that describes the conformation of the block copolymer chain in the microphase separated state.<sup>22</sup> This conformation, and thus the preferred interfacial curvature, is determined by the minimization of the sum of interfacial enthalpy and chain stretching entropy components of the free energy under the constraints that the chains must fill space to uniform density. The observation of the wormlike micelle structure in the I<sub>2</sub>S block copolymer at equilibrium indicates that the system prefers a curved interface with the two PI blocks on the concave side. The kinetically trapped, folded-sheet lamellar system, produced by casting in a selective

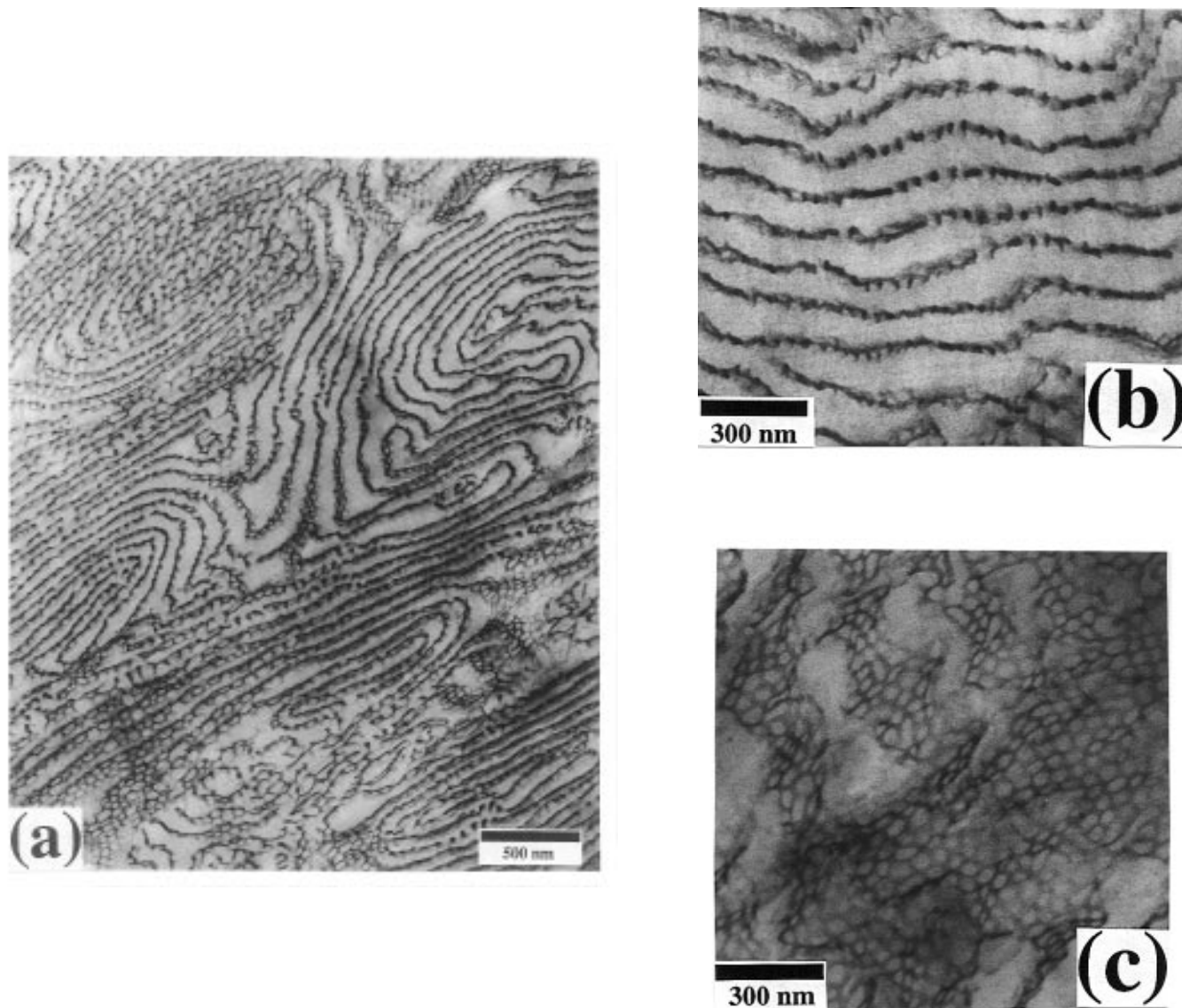


**Figure 6.** (a) TEM micrograph of cyclohexane-cast I<sub>2</sub>S-81 annealed at 120 °C for 1 week. The sample displays the intermediate structure of dark PI layers of folded-lace embedded in a continuous light PS matrix. (b) TEM micrograph at a higher magnification displaying a projection parallel to the layers of folded lace. (c) TEM micrograph displaying a projection predominantly perpendicular to the folded lace.

solvent, forces the I<sub>2</sub>S molecules to accommodate a flat interface. Since this is not the preferred interfacial curvature for these molecules, the sum of interfacial and chain stretching energies will not be minimized. These nonequilibrium chain conformations provide the stored energy that drives the transition back to wormlike micelles once the system is heated in the vacuum oven and thus given the mobility to rearrange.

The first annealing temperature employed, 120 °C, is high enough to allow the system molecular mobility and still put the system in the strong segregation regime. Thus, the system does not have the option of disordering and re-forming the equilibrium structure. Instead, the system must find a kinetic pathway for the transition from lamella to the ROW phase that keeps the strongly segregated interface intact except for localized, discontinuous breaks or jumps. The TEM micrographs in Figure 6 indicate how this is accomplished. Upon annealing, the local driving force for each chain to experience a preferred interfacial curvature with the PI chains on the concave side results in an undulation of the lamellar layers. This undulation builds in amplitude until the PI layers actually become

perforated by PS channels. The point at which interfacial undulations poke through the PI layers to form holes represents a localized discontinuous break in the otherwise continuously deforming and evolving interfacial structure. The PI branches which separate the holes in the PI layers relax and become like a mesh or lace of interconnected cylinders. In so doing, they approach their preferred interfacial curvature. Several groups have observed equilibrium morphologies in different systems similar to the folded-lace intermediate structure. In their study of order–order transitions in low molecular weight diblock copolymers, Khandpur et al.<sup>23</sup> observed an equilibrium “hexagonally perforated lamellar” phase, or HPL, in the weakly to intermediately segregated (high temperature and low  $\chi N$ ) regime. The HPL phase consists of alternating layers of PI and PS in which the PS layers are perforated by PI channels in hexagonal symmetry. Disko et al.<sup>24</sup> have observed a “catenoid lamellar” phase, identical in structure to the HPL phase, in a strongly segregated blend of PS/PI diblock and PS homopolymer with the PS forming the channels through the PI layers. Also in a blend system of PS/PI, specifically utilizing (AB)<sub>n</sub> four-arm starblock



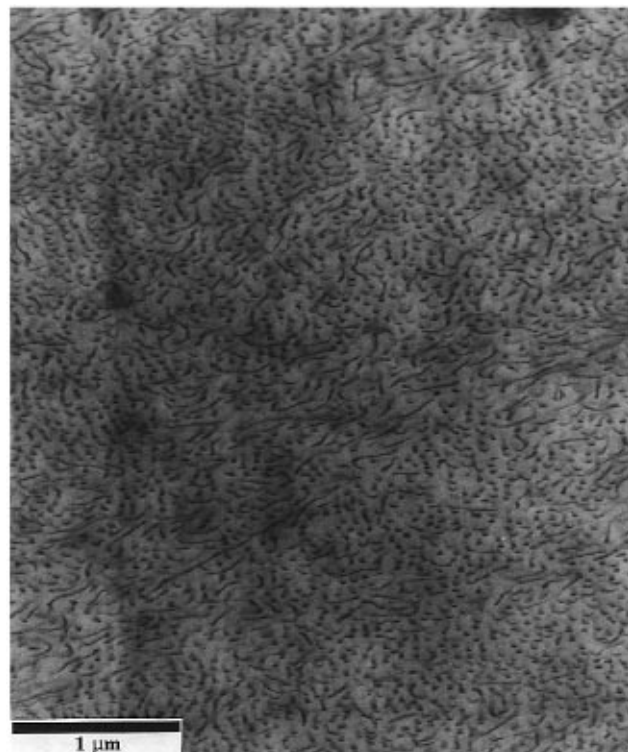


**Figure 7.** TEM micrograph of cyclohexane-cast  $I_2S-81$  displaying the randomly oriented worm, or ROW, phase after annealing at 125 °C for 20 days (also representative of the samples annealed at 150 °C).

copolymers and PS homopolymer, Hashimoto et al.<sup>1</sup> observed a "mesh" phase. This mesh phase most resembles the folded-lace structure in that the PS channels through the alternating PI layers do not occur in a hexagonal symmetry and fluctuate slightly in shape and size. While all of these morphologies resemble the folded-lace structure observed in this work, the folded lace is inherently thermodynamically unique. All of the above phases represent *equilibrium* states of the respective systems whether they are weakly segregated, neat diblocks at high temperatures, or strongly segregated blends at room temperature. To our knowledge, a quenched, *intermediate* layered-lace microstructure has never been observed in a neat, strongly segregated block copolymer system.

The prolonged, high-temperature annealing experiments conducted on the cyclohexane-cast samples allow the observation of the full transition: folded sheets, through folded lace, and eventually all the way back to the randomly oriented worm phase, or ROW. The prolonged annealing at 125 and 150 °C for 20 days allowed sufficient time and thermal energy for the system to relax into its equilibrium wormlike structure and erase the kinetically trapped nonequilibrium chain conformations. Figure 7 is a TEM micrograph of the cyclohexane-cast material after the extended annealing treatment at 125 °C. The results of the 150 °C annealing treatment are identical to the behavior represented in Figure 7. The entire morphological transformation is schematically represented in Figure 8. Originally, the samples displayed the folded lamellar morphology as shown in Figure 5. Identical results were also obtained for folded-lace intermediate samples which were already previously annealed at 120 °C for 1 week. Both the folded-lamellar structure and the intermediate folded-lace structure transformed into ROW phases almost identical to that formed when cast and annealed

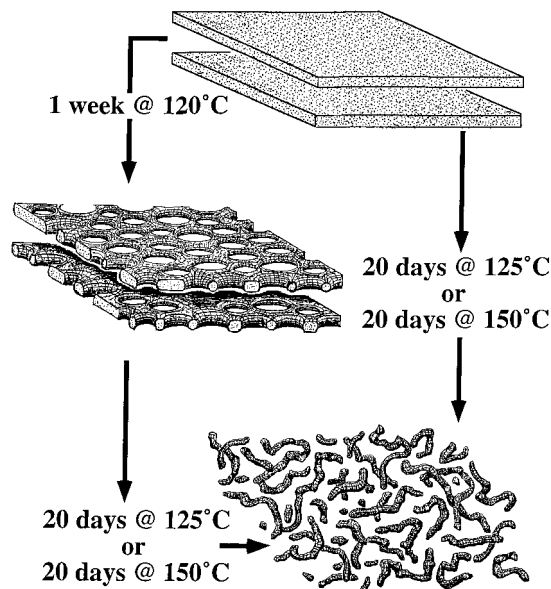


**Figure 8.** Schematic of the entire  $I_2S-81$  morphological transition: selective solvent-cast alternating layers of PI and PS through the folded-lace intermediate and finally reaching the ROW equilibrium phase.

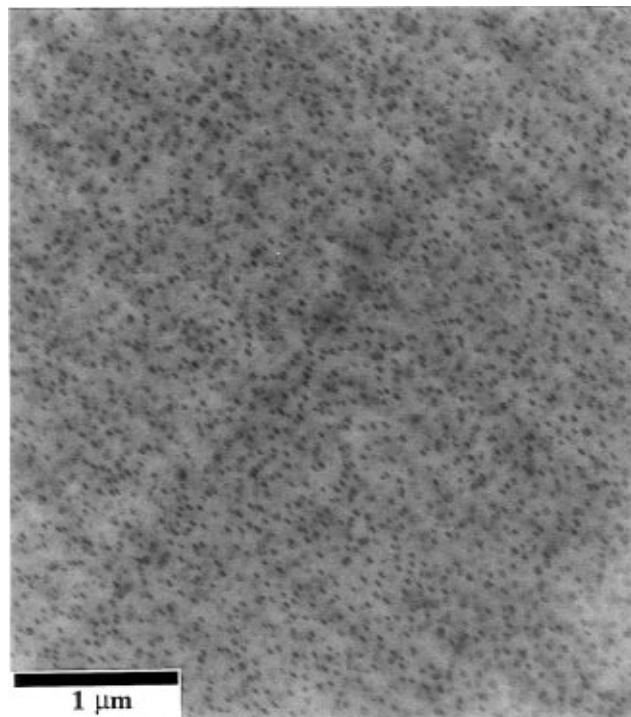


**Figure 9.** TEM micrograph of dioxane-cast  $I_2S-81$  after annealing at 120 °C for 1 week displaying kinetically trapped spherical PI micelles in a PS matrix.

from the nonpreferential solvent toluene. The PI worms produced by annealing the folded-sheet structure appear more uniform in their shape and distribution in space since they originated from the well-ordered, nonequilibrium layered structure as opposed to a nonpreferentially solvated, homogeneous state. The transformation of both the original folded-lamellar structure and the folded-lace intermediate into essentially identical ROW phases supports the equilibrium nature of this novel, randomly oriented block copolymer phase.

Figure 9 is a TEM micrograph of dioxane-cast  $I_2S-81$ , both before and after the initial annealing treatment at 120 °C for 1 week. The system microphase separated

into a spherical micelle structure with dark PI spherical domains lying in a continuous matrix of PS. Just as in the cyclohexane-cast sample, as the system microphase separated the solvent was partitioned unequally between the PS domains and PI domains. Therefore, the PS microphase had an effectively larger volume fraction due to its swelling by the selective solvent forcing the PI blocks into the cores of the spherical micelles. When the remaining solvent evaporated, the morphology was kinetically trapped somewhere within the spherical region of the phase diagram in Figure 4. However, this spherical nonequilibrium phase is unlike the nonequilibrium cyclohexane-cast samples. Because the selective solvent-cast PI domains make up a dispersed structure, it is essentially impossible for them to link together to form a less dispersed morphology such as cylinders, worms, or lamella even though such a transition might be energetically favorable. The PS coronas of these spherical micelles screen the PI cores from one another, preventing them from joining together to produce more continuous PI domain structures. A thermoreversible order–order transition has been observed between cylinders and spheres in a weakly to intermediately segregated, low molecular weight PS/PI diblock.<sup>25</sup> While the transition from hexagonally packed cylinders to spheres only took between 30 and 60 min to occur, the opposite transition required ~40 h. Only at very high temperatures, placing the system in the intermediate or weak segregation limit where order–order transitions can occur, could large chain conformational changes take place and the unfavorable enthalpic interactions be significantly lowered so that the spherical micelles could link and form the equilibrium ROW phase.

## Conclusions

A unique, randomly oriented worm micelle morphology, or ROW, is observed in an I<sub>2</sub>S simple graft block copolymer with  $\phi_s = 0.81$ . Via a set of selective solvent casting and prolonged, high-temperature annealing experiments, combined with experimental results utilizing a nonselective solvent, this morphology was demonstrated to be the equilibrium state for the system. The worm structure occurs only at or near the particular volume fraction where the two PI backbone chains per molecule are first forced to the concave side of the PS/PI interface in the microphase separated state. In another paper, Pochan et al.<sup>3</sup> find two other I<sub>2</sub>S samples, one with a slightly higher PS graft volume fraction ( $\phi_s = 0.89$ ) and one with a slightly lower PS volume fraction ( $\phi_s = 0.66$ ), which form a hexagonally packed PS cylindrical phase and alternating PS/PI lamellar phase, respectively. While both of these phases were predicted theoretically, the volume fraction window in which the ROW phase resides is predicted to be a bicontinuous phase.<sup>2</sup> The ROW phase does not necessarily preclude the existence of the theoretically predicted bicontinuous phase. However, the above experiments support the premise that the wormlike micelle morphology is an equilibrium structure which exists due to the novel graft

architecture of the molecule and the unique relationship between the particular volume fraction of  $\phi_s = 0.81$  and the concavity of the PS/PI interface on which the two PI chains per molecule must reside.

**Acknowledgment.** D.J.P., S.P.G., S.P., and J.W.M. acknowledge funding from the Army Research Office under Contract DAAHO4-94-G-0245. D.J.P. thanks J. David for the use of the high-vacuum line. Additionally, S.P.G. acknowledges an Army Young Investigator Award DAAH04-95-I-0305. We acknowledge the use of TEM instrumentation in the W. M. Keck Polymer Morphology Laboratory at the University of Massachusetts—Amherst, as well as instrumentation support from the Materials Research Science and Engineering Center at the University of Massachusetts.

## References and Notes

- (1) Hashimoto, T.; Koizumi, S.; Hasegawa, H.; Izumitani, T.; Hyde, S. T. *Macromolecules* **1992**, *25*, 1433.
- (2) Milner, S. T. *Macromolecules* **1994**, *27*, 2333.
- (3) Pochan, D. J.; Gido, S. P.; Pispas, S.; Mays, J. W.; Ryan, A. J.; Fairclough, P.; Hamley, I. W.; Terrill, N. *Macromolecules*, in press.
- (4) Kinning, D. J.; Winey, K. I.; Thomas, E. L. *Macromolecules* **1988**, *21*, 3502.
- (5) Jung, K.; Abetz, V.; Stadler, R. *Macromolecules* **1996**, *29*, 1076.
- (6) Hadjichristidis, N.; Iatrou, H.; Behal, S. K.; Chludzinski, J. J.; Disko, M. M.; Garner, R. T.; Liang, K. S.; Lohse, D. J.; Milner, S. T. *Macromolecules* **1993**, *26*, 5812.
- (7) Helfand, E.; Wasserman, Z. R. *Macromolecules* **1976**, *9*, 879.
- (8) Semenov, A. N. *Sov. Phys. JETP* **1985**, *61*, 733.
- (9) *Polymer Handbook*, 2nd ed.; Brandrup, J., Immergut, E. H., Eds.; Wiley Interscience: New York, 1975.
- (10) *Handbook of Polymer-Liquid Interaction Parameters & Solubility Parameters*; Barton, A. F. M., Ed.; CRC Press: Boston, 1990.
- (11) Hashimoto, T.; Nagatoshi, K.; Todo, A.; Hasegawa, H.; Kawai, H. *Macromolecules* **1974**, *7*, 364.
- (12) Thomas, E. L.; Kinning, D. J.; Alward, D. B.; Henkee, C. S. *Macromolecules* **1987**, *20*, 2934.
- (13) Winey, K. I.; Thomas, E. L.; Fetters, L. J. *Macromolecules* **1991**, *24*, 6182.
- (14) Owens, J. N.; Gancarz, I. S.; Koberstein, J. T.; Russell, T. P. *Macromolecules* **1989**, *22*, 3380.
- (15) Mori, K.; Hasegawa, H.; Hashimoto, T. *Polym. J.* **1985**, *17*, 799.
- (16) Rounds, N. A. Ph.D. Dissertation, University of Akron, 1970.
- (17) Leibler, L. *Macromolecules* **1980**, *13*, 1602.
- (18) Olvera de la Cruz, M.; Sanchez, I. C. *Macromolecules* **1986**, *19*, 2501.
- (19) Fogden, A.; Hyde, S. T.; Lundberg, G. *J. Chem. Soc., Faraday Trans.* **1991**, *87*, 949.
- (20) Hyde, S. T. *Colloq. Phys.* **1990**, *C7*, 209.
- (21) Israelachvili, J. N. *Intermolecular and Surface Forces*, 2nd ed.; Academic Press: New York, 1992.
- (22) Olmsted, P. D.; Milner, S. T. *Phys. Rev. Lett.* **1994**, *72*, 936.
- (23) Khandpur, A. K.; Foerster, S.; Bates, F. S.; Hamley, I. W.; Ryan, A. J.; Bras, W.; Almdal, K.; Mortensen, K. *Macromolecules* **1995**, *28*, 8796.
- (24) Disko, M. M.; Liang, K. S.; Behal, S. K.; Roe, R. J.; Jeon, K. J. *Macromolecules* **1993**, *26*, 2983.
- (25) Sakurai, S.; Kawada, H.; Hashimoto, T.; Fetters, L. J. *Macromolecules* **1993**, *26*, 5796.
- (26) Bates, F. S.; Frederickson, G. H. *Annu. Rev. Phys. Chem.* **1990**, *41*, 525.

MA9601225